Z. Phys. Chem. **222** (2008) 1225–1245 / **DOI** 10.1524/zpch.2008.5385

NMR Study of Blue-Shifting Hydrogen Bonds Formed by Fluoroform in Solution

By Nikolai S. Golubev[1], Gleb S. Denisov[1], Sven Macholl[1,2], Sergei N. Smirnov[1], Ilja G. Shenderovich[1,2], and Peter M. Tolstoy[1,2,*]

[1] V.A. Fock Institute of Physics, St. Petersburg State University, Russia.
[2] Institute of Chemistry and Biochemistry, Free University of Berlin, Germany

Dedicated to Prof. Dr. Hans-Heinrich Limbach on the occasion of his 65th birthday

(Received March 7, 2008; accepted April 10, 2008)

Blue Shifting Hydrogen Bond / Fluoroform / Low-Temperature NMR

Low-temperature (193 K) ^{1}H, ^{13}C and ^{15}N NMR spectra of blue- and red-shifting H-bonded complexes formed by fluoroform with various proton acceptors were measured. Experimental NMR parameters were plotted versus the *ab initio* calculated H-bond strength (MP2/6–31+G(d, p); interaction energy varies from ~5 up to 25 kJ · mol^{-1} in the series). We show that experimental ^{1}H and ^{15}N shieldings, as well as the H/D isotope effect on ^{13}C shielding change monotonously with the calculated H-bond strengthening. The ^{13}C chemical shift and the CH scalar coupling change non-monotonously and the extremum points are situated approximately in the region of transformation from blue- to red-shifting H-bonds. The most informative NMR feature is the H/D isotope effect on ^{15}N shielding which changes its sign upon transformation from blue- to red-shifting H-bonds.

To rationalize these observations, *ab initio* calculations of ^{13}C and ^{15}N shieldings as functions of C···H and C···N distances were performed for complexes of CHF_3 with acetonitrile (blue-shifting) and pyridine (red-shifting). The coupling of the vibrations of the covalent and hydrogen bonds has been accounted for by direct computation of the distance C···N = *f*(C···H) dependence. We demonstrate that the unusual sign of the H/D isotope effect on ^{15}N chemical shift across a blue-shifting H-bond can be explained as a result of the inversion of the dynamic coupling of two vibrations.

1. Introduction

Very weak hydrogen bonds formed by a number of CH acids with weak proton acceptors often exhibit rather non-conventional behaviour in vibrational spectra,

* Corresponding author. E-mail: tolstoy@chemie.fu-berlin.de, peter.tolstoy@pobox.spbu.ru

namely, a high frequency (blue) shift for the CH stretching vibrational bands [1–11]. The blue shift of the vibrational frequency is usually accompanied by a considerable intensity decrease of the corresponding IR absorption vibrational band. It should be noted that these two spectroscopic features are linked, but only indirectly. Indeed, the frequency shift is determined by the shape of the potential energy surface as a function of vibrational coordinates, while the intensity change originates from the shape of the dipole moment function. In particular, for several complexes of fluoroform with nitrogen bases ($F_3CH\cdots N(CH_3)_3$, e.g.) a strong decrease in intensity of the CH stretching band (ν_1 for the CHF_3 molecule), which exhibits a small but conventional frequency red shift, was reported [9, 12]. In Ref. [9] such hydrogen bonds are termed "pseudo blue-shifting" ones. Quantum-mechanical calculations (*ab initio* as well as DFT) show also some shortening of the CH bonds as a result of forming blue-shifting H-bonds [1, 3, 4, 5, 7, 13–17]. In contrast, usual red-shifting H-bonds are characterised by some lengthening of the CH bonds.

The unusual geometric and spectroscopic properties of the weak CH interactions with proton acceptors led to several terminological disputes. Some authors doubt that the term "hydrogen bond" is an appropriate one [18], while the others have introduced the term "anti-hydrogen bond" [19]. Throughout this paper we will use the most widely accepted term "blue-shifting hydrogen bond".

To the best of the authors' knowledge, experimental studies of such complexes have been performed mainly using IR spectroscopy. Another technique which usually provides valuable information on hydrogen bonding, is NMR spectroscopy. However, there is only few data published about the NMR manifestations of blue-shifting hydrogen bonds [14]. The goal of the present research is to find any characteristic features of the improper type of H-bonding in NMR spectra.

We have studied CHF_3 and CDF_3 molecules in gaseous phase (**1**), in neat liquid (**2**), dissolved in ethyl chloride-d_5 (CD_3CD_2Cl) (**3**), and in CD_2Cl_2 solution in complexes with the following proton acceptors (bases): acetonitrile-d_3 (CD_3CN) (**4**), 4-methoxybenzonitrile (p-MeO-PhCN) (**5**), dimethylether-d_6 ($(CD_3)_2O$) (**6**), 4-dimethylaminobenzonitrile (p-Me_2N-PhCN) (**7**), acetone-d_6 ($(CD_3)_2CO$) (**8**), pyridine-d_5 (C_5D_5N) (**9**), trimethylamine-d_9 ($(CD_3)_3N$) (**10**) and 2, 4, 6-trimethylpyridine (2, 4, 6-Me_3-C_5H_2N) (**11**). Schematic structures of the complexes are shown in Scheme 1. Usage of deuterated bases allowed us to avoid intensive background signals in ^1H NMR spectra. To obtain ^{15}N NMR spectra, non-deuterated nitrogen bases enriched with ^{15}N isotope were used: acetonitrile-^{15}N (**4N**), 4-methoxybenzonitrile-^{15}N (**5N**), 4-dimethylaminobenzonitrile-^{15}N (**7N**), pyridine-^{15}N (**9N**) and 2, 4, 6-trimethylpyridine-^{15}N (**11N**), see Experimental section for details. According to previously published IR and computational data, the successive H-bond strengthening in these complexes is accompanied by the transformation of the hydrogen bond from the blue-shifting to the conventional red-shifting [8, 9, 20] (see Table 1).

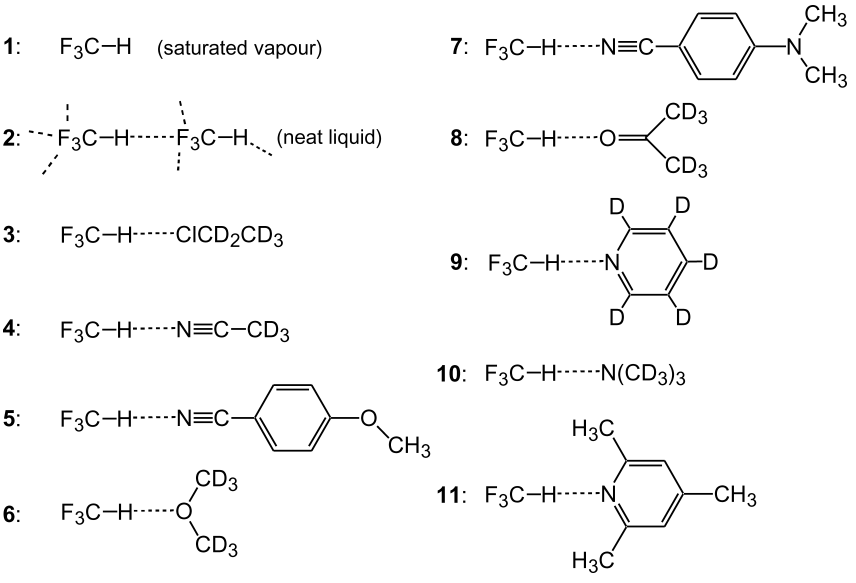

Scheme 1. Schematic structures of the complexes of fluoroform, studied in this work.

In particular, the CH stretching frequency of the CHF_3 dissolved in neat CD_3CN is shifted to higher frequency by 10.8 cm^{-1} in comparison with that of free CHF_3 in the gas phase (blue shift). When CHF_3 is dissolved in deuterated pyridine, C_5D_5N, which is a stronger proton acceptor, the CH frequency shift is -1.2 cm^{-1}. When the proton accepting ability of the base increases even further, as in $(CD_3)_3N$, the CH stretching shift of -21.2 cm^{-1} has been measured (red shift).

In this work, low-temperature (193 K) ^1H, ^{13}C and, for nitrogen bases (except for trimethylamine), ^{15}N NMR spectra were recorded. These provided chemical shifts, scalar coupling constants between ^1H and ^{13}C and H/D isotope effects on ^{13}C and ^{15}N NMR chemical shifts. In parallel, *ab initio* calculations (MP2/6–31+G(d, p)) of the equilibrium CH distances and the H-bond energies (taken as the difference of full electronic energy of a complex and the corresponding free molecules) were performed. For complexes of CHF_3 with acetonitrile (**4**) and pyridine (**9**) functions of electronic energy and shielding constants on C···H and C···N distances were calculated, as well as the dependence C···N = *f*(C···H).

The discussion of these results is structured as follows. Experimental and computational results are considered together. Firstly, all the considered experimental NMR values are plotted against the calculated H-bond energy and the resulting dependencies are analysed. Secondly, secondary H/D isotope effects on chemical shifts are evaluated within the simplest model, assuming that carbon shielding depends solely on the C···H distance, and nitrogen shielding on the

Table 1. Literature data on the experimental and *ab initio* calculated blue and red shifts of the CH stretching frequency (ν_1) in the series of complexes of fluoroform with bases.

No.	Base	Conditions	ν_1 complex (ν_1 free)/ cm^{-1}	shift/cm^{-1}	Ref.
1	none	gas	3035.2		[20]
	none	liquid Ar	3036.7		[9]
	none	liquid Xe	3030.5		[9]
	none	liquid Kr	3033.0		[8]
2	CHF_3 (dimer)	liquid Kr	3057.0(3033.0)	+24.0	[8]
3	CD_3CD_2Cl [a]				
4	CD_3CN	liquid CD_3CN	3046(3035.2)	+10.8	[20]
5	p-MeO-PhCN [a]				
6	$(CH_3)_2O$	liquid Ar	3054.8(3036.7)	+18.1	[9]
	$(CH_3)_2O$	MP2/6–31+G(d, p)	3287.5(3270.3)	+17.2	[9]
7	p-Me_2N-PhCN [a]				
8	$(CD_3)_2CO$	liquid $(CD_3)_2CO$	3051(3035.2)	+15.8	[20]
9	C_5D_5N	liquid pyridine-d_5	~3034(3035.2)	−1.2	[20]
	C_5H_5N	liquid Xe	3033.3(3030.5)	+2.8	[9]
	C_5H_5N	MP2/6–31+G(d, p)	3266.7(3270.3)	−3.6	[9]
10	$(CD_3)_3N$	liquid $(CD_3)_3N$	3014(3035.2)	−21.2	[20]
	$(CH_3)_3N$	liquid Ar	3013.9(3036.7)	−22.8	[9]
	$(CH_3)_3N$	MP2/6–31+G(d, p)	3219.0(3270.3)	−51.3	[9]
11	2, 4, 6-Me_3-C_5H_2N [a]				

a - no data found in the literature on these complexes

C···N distance. Changes of interatomic distances upon deuteration of the complex are estimated using the linear three-mass model by Sokolov et al. [21, 22] in conjunction with the calculated C···N = *f*(C···H) dependence. Finally, experimental and calculated values of H/D isotope effects on chemical shifts are compared.

2. Experimental

2.1 Synthesis

Fluoroform CHF_3 was prepared by decarboxylation of potassium trifluoroacetate in ethyleneglycol. The product was purified by passing it through H_2SO_4 and repeated distillation at −70 °C under reduced pressure [23]. For the preparation of CDF_3 (~80% ^2H), ethyleneglycol was first of all deuterated (in OH sites) by repeatedly adding and removing D_2O under reduced pressure in a rotor evaporator, then the synthesis was carried out as described above. Commercially available (Aldrich) CD_2Cl_2 (99.9% ^2H), CD_3CD_2Cl (99% ^2H), $(CD_3)_2CO$ (99.9% ^2H), pyridine-d_5 (99% ^2H) and acetonitrile-d_3 (99.8% ^2H) were used without addi-

tional purification. Dimethylether $(CD_3)_2O$ (99% ^2H) was synthesized from methanol-d_3 and H_2SO_4 by a standard technique. Non-deuterated nitrogen bases enriched with ^{15}N isotope (acetonitrile-^{15}N, 4-metoxy- and 4-dimethylamino-benzonitriles-^{15}N, pyridine-^{15}N and 2, 4, 6-trimethylpyridine-^{15}N) were prepared and purified according to Ref. [24]. Trimethylamine-d_9 was synthesized according to Ref. [25].

2.2 Sample preparation

The samples were prepared in hermetic thick-walled NMR sample tubes equipped with PTFE valves (Wilmad) that withstand gas pressure up to ~40 bar. The tubes were filled with fluoroform on a high vacuum line and the solvents were added via vacuum transfer. The technique of low temperature NMR with liquefied gases as solvents has been described in [26].

The sample of **1** was the saturated vapour above the liquid CHF_3 (or CDF_3). The sample of **2** was neat fluoroform (CHF_3 or CHF_3/CDF_3 mixture). The sample of **3** was a 0.05 mol · L^{-1} solution of 20% CHF_3 + 80% CDF_3 in CD_3CD_2Cl (to measure a good signal-to-noise natural abundance ^{13}C NMR spectrum the overall concentration of fluoroform was increased to 0.2 mol · L^{-1}). To measure ^1H and ^{13}C NMR spectra of **4–11** first the 1 mol · L^{-1} solutions of the corresponding bases in CD_2Cl_2 were prepared directly in the sample tubes, then mixtures of CHF_3 and CDF_3 were added (overall concentration of fluoroform was 0.05 mol · L^{-1}). Deuterated nitrogen bases were used if available to avoid very intensive background signals in ^1H NMR spectra. Samples for the measurement of ^{15}N NMR spectra were prepared in a different way: non-deuterated nitrogen bases enriched with ^{15}N isotope were dissolved in a CDF_3/CHF_3 mixture (complexes **4N**, **5N**, **7N**, **9N** and **11N**). Concentration of the base was about 0.05 mol · L^{-1}.

2.3 NMR experiments

Spectra were recorded with a Bruker DPX-300 NMR spectrometer equipped with a low-temperature probe, which in principle allowed us to perform experiments down to the melting point of fluoroform (118 K). However, all experiments were performed at 193 K, because many of the bases were precipitating of the 1 mol · L^{-1} solution in CD_2Cl_2 close to its melting point (176 K). ^1H and ^{13}C NMR chemical shifts were measured using TMS as internal standard (a controlled amount of TMS was added to CD_2Cl_2 prior to the sample preparation). The total deuterium fraction of fluoroform was determined by comparison of the integrated intensity of the CHF_3 proton quartet with that of the TMS protons signal. The proton decoupled ^{15}N NMR spectra consisted of a single line with the position depending on the deuterium fraction of fluoroform. Since this dependence appeared to be practically linear, it allowed us to extrapolate the full H/D isotope effect on ^{15}N chemical shift transmitted across the hydrogen bridge. ^{15}N NMR spectra were referenced to the solutions of the free bases (1 mol · L^{-1}

in CD_2Cl_2) as external standards. Thus, the resulting relative ^{15}N chemical shifts are subject to systematic errors. We note, however, that these systematic errors cancel for the H/D isotope effects on ^{15}N chemical shifts.

2.4 QM computations

The *ab initio* calculations at the MP2 level of theory were performed using the Gaussian 98 package [27]. We have used the standard basis sets 6–31+G(d, p), which has diffuse functions on heavy atoms and a set of polarization functions, both on hydrogen and heavy atoms. The optimized equilibrium geometry and total electronic energy E of **1**–**11** were obtained utilizing the CP-corrected gradient optimization technique. At the same level of theory, the relative magnetic shielding constants, $\sigma^{rel} = \sigma^{complex} - \sigma^{monomer} = \delta^{monomer} - \delta^{complex}$, were calculated for complexes **1**, **4** and **9** using the GIAO method as functions of internal variables $r = r_{CH} - r_{CH}^{e}$ and $R = R_{CN} - R_{CN}^{e}$, where r_{CH} and R_{CN} are the manually selected C···H and C···N distances, while r_{CH}^{e} and R_{CN}^{e} are the C···H and C···N interatomic distances in equilibrium (fully optimized) geometry of the corresponding system. All other variables were kept constant.

The normal coordinate analysis procedure included in the Gaussian 98 gave unreliable results for intermolecular vibrations and was therefore replaced by the following procedure. The force constants required for estimating the geometric isotope effects were calculated in one-dimensional approximation based on fitting the obtained curves, $E = f(r)$ and $E = f(R)$, with 3^{rd} power polynomials. Moreover, for complexes **4** and **9** the dependencies $R = f(r)$ were calculated as described in [28].

2.5 Nomenclature

In this paper we use the following nomenclature: chemical shifts are labelled as $\delta(\underline{C}L\cdots X)$, where the observed nucleus is underlined, L = H, D and X is the proton accepting atom, which can be N (**4**, **5**, **7**, **9**, **10**, **11**), O (**6**, **8**), F (**2**), Cl (**3**) or absent (**1**). For example, the nitrogen chemical shift of the deuterated complex **4** is be labelled as $\delta(CD\cdots\underline{N})$. The complex to which the chemical shift refers will be clear from the context. A similar nomenclature is used for the coupling constants, e.g. $^{1}J(\underline{C}L\cdots X)$.

3. Results

3.1 ^{1}H and ^{13}C NMR experiments

For brevity, the primary experimental material will be presented here only for complex **3**. ^{1}H and ^{13}C NMR spectra for other complexes are qualitatively similar. In the bottom of Fig. 1 the ^{1}H NMR spectrum of the sample containing a 0.05 mol · L^{-1} solution of fluoroform in CD_3CD_2Cl is shown. The signal of

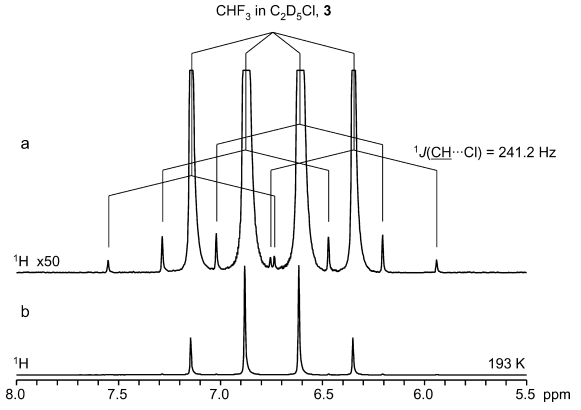

Fig. 1. ^{1}H NMR spectrum of a solution containing 0.05 mol · L^{-1} CHF_3 in CD_3CD_2Cl at 193 K.

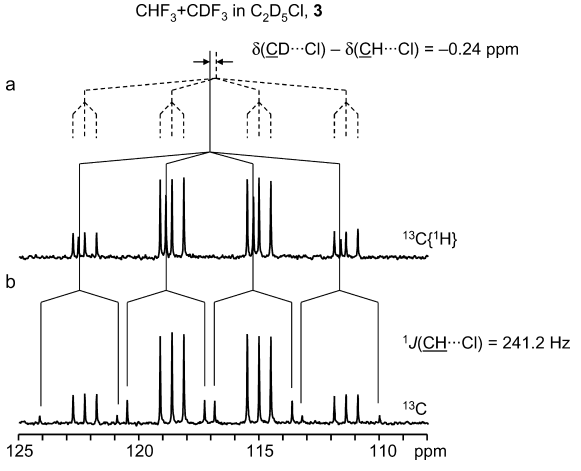

Fig. 2. Natural abundance proton decoupled (a) and proton coupled (b) ^{13}C spectra of a solution containing 20 % CHF_3 + 80 % CDF_3 (overall concentration 0.2 mol · L^{-1}) dissolved in CD_3CD_2Cl at 193 K.

CHF_3 at δ(C**H**···Cl) = 6.69 ppm is split into a quartet due to the scalar interaction with three ^{19}F spins. The coupling constant ^{1}J(C**H**···Cl) = 241.2 Hz can be measured using the ^{13}C satellites, shown on top of Fig. 1.

In Fig. 2, low-field parts of the proton decoupled (Fig. 2a) and proton coupled (Fig. 2b) natural abundance ^{13}C spectra of a solution containing 0.2 mol · L^{-1} of the mixture 80 % CDF_3 + 20 % CHF_3 in CD_3CD_2Cl are shown. Signals of CHF_3 and CDF_3 are split into quartets due to the scalar coupling between ^{13}C and ^{19}F spins. Additionally, the carbon signal of CHF_3 is split into

Table 2. Experimental ^{1}H and ^{13}C NMR parameters of complexes formed by CHF_3 and CDF_3 with proton acceptors.

No.	Base	$\delta(\underline{C}H\cdots X)/$ ppm	$\delta(\underline{C}H\cdots X)/$ ppm	$\delta(\underline{C}D\cdots X)/$ ppm	$\delta(\underline{C}D\cdots X) - \delta(\underline{C}H\cdots X)/$ ppm	$^{1}J(\underline{C}H\cdots X)/$ Hz
1	none [a]	6.21	118.84	118.62	−0.22	235.1
2	CHF_3 (liquid)	6.39	118.60	118.36	−0.24	238.0
3	CD_3CD_2Cl	6.69[b]	118.26[c]	118.02[c]	−0.24[c]	241.2[b]
4	CD_3CN [d]	6.73	118.15	117.87	−0.28	244.9
5	p-MeO-PhCN [d]	7.18	117.96	117.66	−0.30	245.9
6	$(CD_3)_2O$ [d]	7.11	117.95	117.65	−0.30	246.1
7	p-Me_2N-PhCN [d]	7.39	117.90	117.58	−0.32	246.7
8	$(CD_3)_2CO$ [d]	7.37	117.94	117.62	−0.32	246.4
9	C_5D_5N [d]	7.54	117.91	117.64	−0.27	246.3
10	$(CD_3)_3N$ [d]	7.32	118.01	117.63	−0.38	245.2
11	2, 4, 6-Me_3-C_5H_2N [d]	7.72	118.32	117.86	−0.46	243.2

a - experimental data for the saturated vapor over liquid fluoroform layer at 273 K.
b - 0.05 mol · L^{-1} CHF_3/CDF_3 added to the neat base at 193 K.
c - 0.2 mol · L^{-1} CHF_3/CDF_3 added to the neat base at 193 K.
d - 0.05 mol · L^{-1} CHF_3/CDF_3 added to the 1 mol · L^{-1} solution of a base in CD_2Cl_2 at 193 K.

a doublet, $^{1}J(\underline{C}H\cdots Cl)$ = 241.2 Hz. The centres of multiplets in the ^{13}C NMR spectra with CHF_3 and CDF_3 do not coincide. This secondary isotope effect on the ^{13}C chemical shift is $\delta(\underline{C}D\cdots Cl) - \delta(\underline{C}H\cdots Cl) = -0.24$ ppm.

In Table 2 ^{1}H and ^{13}C NMR parameters obtained for all complexes are listed.

3.2 ^{15}N NMR experiments

Again, for brevity we present here the primary experimental material only for the representative complexes **4N** and **9N**. In Fig. 3a, the ^{15}N NMR spectrum of 0.05 mol · L^{-1} solution of $CH_3C^{15}N$ in CHF_3 is shown. After deuterating the solvent to 80 % the ^{15}N signal is somewhat shifted high field (Fig. 3b). Linear extrapolation to the 100 % deuterated solvent, i.e. 100 % CDF_3 (Fig. 3c), gives the full value of the secondary H/D isotope effect on the ^{15}N chemical shift in complex **4N**, $\delta(CD\cdots\underline{N}) - \delta(CH\cdots\underline{N}) = -0.16$ ppm.

In Fig. 3d and 3e the ^{15}N NMR spectra of 0.05 mol · L^{-1} solutions of $C_5H_5{}^{15}N$ in CDF_3 + CHF_3 mixtures are shown. Again, extrapolation to the fully deuterated solvent (Fig. 3f) gives the isotope effect value $\delta(CD\cdots\underline{N}) - \delta(CH\cdots\underline{N}) = +0.25$ ppm for complex **9N**.

In Table 3 ^{15}N NMR parameters obtained for complexes **4N**, **5N**, **7N**, **9N** and **11N** are listed.

3.3 QM calculations of H-bond geometries and energies

In Table 4 the following *ab initio* calculated values are shown: the full electronic energies of the complexes ($E_{complex}$), the full electronic energies of the free bases

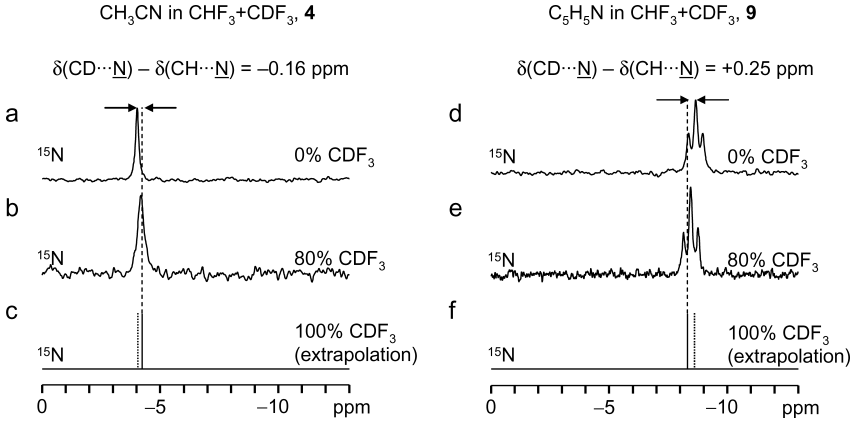

Fig. 3. ^{15}N NMR spectra of the samples containing 0.05 mol · L^{-1} solution of a) $CH_3C^{15}N$ in CHF_3; b) $CH_3C^{15}N$ in mixture 80 % CDF_3 + 20 % CHF_3; d) $C_5H_5{}^{15}N$ in CHF_3; e) $C_5H_5{}^{15}N$ in mixture 80 % CDF_3 + 20 % CHF_3. c) Extrapolated position of ^{15}N signal of 0.05 mol · L^{-1} solution of $CH_3C^{15}N$ in 100 % CDF_3. f) Extrapolated position of ^{15}N signal of 0.05 mol · L^{-1} solution of $C_5H_5{}^{15}N$ in CDF_3. Spectra are referenced to the ^{15}N signal of 1 mol · L^{-1} solution of the corresponding base in CD_2Cl_2 as external standard.

Table 3. ^{15}N chemical shifts for a number of nitrogen bases dissolved in CHF_3 and CDF_3 at 193 K. Chemical shifts are references to the 1 mol · L^{-1} solution of the corresponding nitrogen base in CD_2Cl_2 at 193 K.

No.	Base	δ(CH···N) /ppm [a]	δ(CD···N) /ppm [b]	$\Delta_{DH}\delta_N$ /ppm
4	CH_3CN	−4.63	−4.79	−0.16
5	p-MeO-PhCN	−6.99	−7.04	−0.06
7	p-Me_2N-PhCN	−8.41	−8.38	+0.03
9	C_5H_5N	−9.98	−9.73	+0.25
11	2, 4, 6-Me_3-C_5H_2N	−13.14	−12.83	+0.31

a - 0.05 mol · L^{-1} of the base dissolved in neat CHF_3
b - 0.05 mol · L^{-1} of the base dissolved in neat CDF_3 (extrapolated from ^{15}N chemical shifts measured for CHF_3/CDF_3 mixture)

(E_{base}) interaction energies ΔE (taken as a difference between electronic energies of a complex, AH···B, and two free molecules, AH and B), equilibrium C···H distances, $r_{CH}{}^e$, and dipole moments (μ). The plot $r_{CH}{}^e = f(\Delta E)$ is depicted in Fig. 4 and is discussed below.

3.4 QM calculations of shielding functions

The calculated relative (with respect to the values for the free molecules) ^{13}C shielding constants for systems **1** and **4** as functions of internal coordinate $r = r_{CH} - r_{CH}{}^e$ are listed in Table 5.

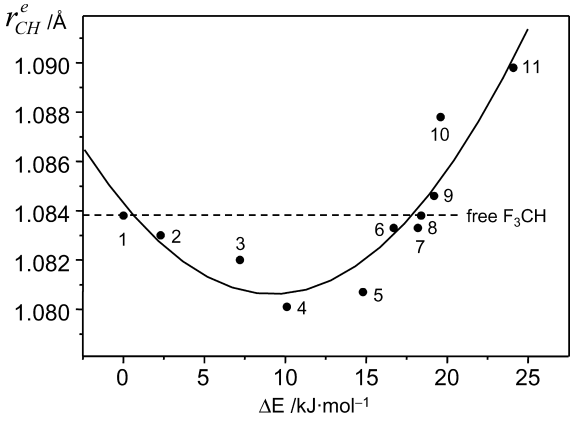

Fig. 4. The calculated equilibrium C···H distance, r_{CH}^e, plotted against the interaction energy ΔE, for fluoroform complexes with different bases. Level: MP2/6–31+G(d, p). The numbering of the complexes corresponds to Scheme 1 and Table 2.

Table 4. *Ab initio* calculated (MP2/6–31+G(d, p)) values of the full electronic energy of the complex ($E_{complex}$), full electronic energy of the free base (E_{base}), interaction energy $\Delta E = -(E_{complex} - E_{base} - E_{CHF3})$, equilibrium C···H distance (r_{CH}^e) and dipole moments (μ) for complexes formed by CHF_3 with various proton acceptors (bases).

No.	Base	$E_{complex}$/ Hartree	E_{base}/ Hartree	ΔE/ Hartree	ΔE/kJ · mol^{-1}	r_{CH}^e/Å	μ/D
1	None	−337.62641			0	1.0838	2.05(1.64[b])
2	CHF_3[a]	−675.25370	−337.62641	0.00088	2.3	1.0830	3.82
3	CD_3CD_2Cl	−524.97473	−187.34558	0.00274	7.2	1.0820	4.74
4	CD_3CN	−453.38626	−115.75604	0.00381	10.1	1.0801	7.13(6.94[b])
5	p-MeO-PhCN	−844.35320	−506.72115	0.00564	14.8	1.0807	8.43
6	$(CD_3)_2O$	−654.57365	−316.94088	0.00636	16.7	1.0833	3.91
7	p-Me_2N-PhCN	−924.64352	−587.01018	0.00693	18.2	1.0833	8.61
8	$(CD_3)_2CO$	−664.12065	−326.48723	0.00701	18.4	1.0838	5.35
9	C_5D_5N	−585.43899	−247.80527	0.00731	19.2	1.0846	5.11
10	$(CD_3)_3N$	−667.09618	−329.46231	0.00746	19.6	1.0878	4.54
11	2, 4, 6-Me_3-C_5H_2N	−983.50823	−645.87264	0.00918	24.1	1.0898	6.44

a - calculated for CHF_3 dimer
b - MP2/6–311++G(3df, 3pd)

In Table 6 the relative ^{15}N shielding constant for complexes **4** and **9** as functions of coordinate $R = R_{CN} - R_{CN}^e$ are collected. For details of calculations see Experimental section. Obtained dependencies are discussed below.

Table 5. *Ab initio* calculated (MP2/6–31+G(d, p)) relative (with respect to the values for the free molecules) ^{13}C shielding constants for systems **1** and **4** as functions of internal coordinate $r = r_{CH} - r_{CH}^{e}$.

$r = r_{CH} - r_{CH}^{e}$, Å	$\sigma^{rel} = \sigma^{complex} - \sigma^{monomer}$	
	1	**4**
−0.025	0.4032	1.5035
−0.020	0.3264	1.4857
−0.015	0.2477	1.3500
−0.010	0.1670	1.1964
−0.005	0.0844	0.9607
0	0	0.6110
0.005	−0.0862	−0.0178
0.010	−0.1535	−0.7821
0.015	−0.2428	−1.5678
0.020	−0.3357	−2.4142
0.025	−0.4107	−3.0357
0.030	−0.5013	−3.3678

Table 6. *Ab initio* calculated (MP2/6–31+G(d, p)) relative (with respect to the values for the free molecules) ^{15}N shielding constants for systems **4** and **9** as functions of internal coordinate $R = R_{CN} - R_{CN}^{e}$.

$R = R_{CN} - R_{CN}^{e}$, Å	$\sigma^{rel} = \sigma^{complex} - \sigma^{monomer}$	
	4	**9**
−0.1	15.100	
−0.08	11.810	
−0.06	9.746	
−0.04	7.464	15.832
−0.02	5.906	12.200
0	4.803	9.221
0.02	3.586	6.971
0.04	2.793	5.204
0.06	2.182	3.864
0.08	1.667	3.017
0.1	1.260	2.450
0.14	0.767	1.582
0.18	0.532	1.121

4. Discussion

First, have a look at Fig. 4. The equilibrium C···H distance, r_{CH}^{e}, first decreases and then rises with increasing the interaction energy ΔE. The transformation from blue- to red-shifting hydrogen bonding occurs in the interaction energy region ~17–19 kJ · mol^{-1}. A simplified qualitative explanation of this fact is as

follows. The effect of CH bond contraction is related to the specific shape of the dipole moment function of fluoroform, which increases with CH bond contraction. The hydrogen bond geometry is always optimized for the maximum electronic dipole moment localized on the CH bond via its polarization (mainly electronic, but partially nuclear, too). This increases the interaction energy with the dipole localized on the lone pair of a base. As a result, the interaction of fluoroform with a base leads to the CH bond contraction. However, the dipole-dipole part of the interaction energy dominates only in very weak hydrogen bonds, while a strong hydrogen bond acquires some covalent character. The exchange part of the interaction energy increases with the proton approaching the center between two heavy atoms. As a result, comparatively strong hydrogen bonds formed by fluoroform are not blue-shifting ones any more; in contrast, their formation is accompanied by CH bond stretching. A more detailed evaluation of different contributions to the interaction energy is given in ref. [29].

4.1 ^{1}H and ^{13}C NMR data

Now, have a look at Fig. 5, where the experimental ^{1}H and ^{13}C NMR parameters of the complexes **1**–**11** are plotted versus the *ab initio* calculated interaction energy ΔE. In Fig. 5a, one can see that $\delta(\underline{C}H\cdots X)$ rises monotonously and apparently linearly with the interaction energy. In contrast to this, the carbon chemical shifts $\delta(\underline{C}H\cdots X)$ and $\delta(\underline{C}D\cdots X)$ (Fig. 5c) first pass a minimum and then rise again. (It should be noted that the calculated *ab initio* values of the interaction energy depend crucially on the level of electron correlation account and the used basis set. However, the shapes of the curves shown in Fig. 5 remain unchanged.) The difference, $\delta(\underline{C}D\cdots X) - \delta(\underline{C}H\cdots X)$, i.e., the secondary H/D isotope effect, is negative, which means shielding of the carbon nucleus as a result of the proton replaced by a deuteron. The absolute value of this isotope effect rises monotonously with the interaction energy (see Fig. 5d), with no peculiarity in the region of the transformation of the blue- to red-shifting hydrogen bonding. In Fig. 5b the dependency of the spin-spin coupling constant, $^{1}J(\underline{C}H\cdots X)$, on the calculated hydrogen bond energy is depicted. Qualitatively, it looks similar to the dependency shown in Fig. 5c and the extremum point is practically in the same ΔE region around 17 kJ $\cdot$ mol^{-1}. According to Fig. 4, the transformation from the blue- to the red-shifting hydrogen bond takes place in this region. We conclude that the non-monotonous functions, $\delta(\underline{C}H\cdots X) = f(\Delta E)$ and $^{1}J(\underline{C}H\cdots X) = f(\Delta E)$, could, in principle, serve as an indicator for this transformation. However, to distinguish between the cases of blue- and red-shifting H-bonds for a particular complex, ^{13}C NMR data for a series of complexes together with their relative interaction energies ΔE are required.

The shape of the curve, $\delta(\underline{C}H\cdots X) = f(\Delta E)$, is rationalized by calculation of the carbon shielding constants for a free fluoroform molecule (**1**) and for a typical blue-shifting hydrogen bonded complex, fluoroform-acetonitrile (**4**), as a function of the internal variable $r = r_{CH} - r_{CH}^{e}$ (Fig. 6).

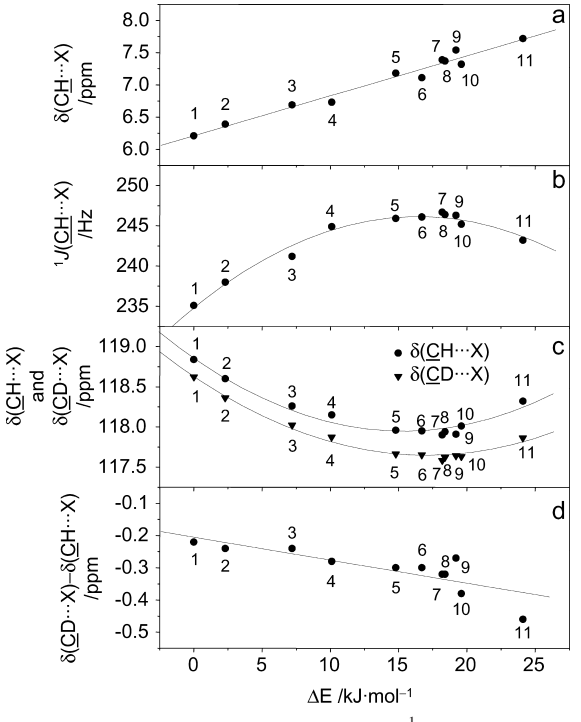

Fig. 5. Experimental values of δ(C$\underline{\text{H}}$···X) chemical shifts (a), ^1J(C$\underline{\text{H}}$···X) coupling constants (b), δ(C$\underline{\text{H}}$···X) and δ(C$\underline{\text{D}}$···X) chemical shifts (c) and δ(C$\underline{\text{D}}$···X) − δ(C$\underline{\text{H}}$···X) isotope effects (d) plotted versus the calculated interaction energy ΔE, for fluoroform complexes with a number of bases. All numerical data are taken from Tables 2 and 4.

The r variable characterizes the CH stretching vibration. The carbon shielding of complex **4** is larger than that of free fluoroform **1** in the region of short C···H distances and decreases with the distance much faster than the shielding of the latter. The observed non-monotonous shape of δ(C$\underline{\text{H}}$···X) = $f(\Delta E)$ for complex **4** may be explained by the competition between the shielding by the neighbouring hydrogen atom and the deshielding by the hydrogen bond itself.

4.2 ^{15}N NMR data

We continue our analysis of experimental NMR data by looking at Fig. 7a, which represents the dependence of the ^{15}N chemical shift of nitrogen bases on the calculated interaction energy. It is seen that the nitrogen chemical shift decreases rapidly with increasing hydrogen bond energy, which is typical for the unsaturated bases, such as nitriles and pyridines [30]. It is well known that nitrogen shielding caused by the complete protonation of such bases can reach the value of as much as 120 ppm. A conventional explanation of this phenomenon in terms

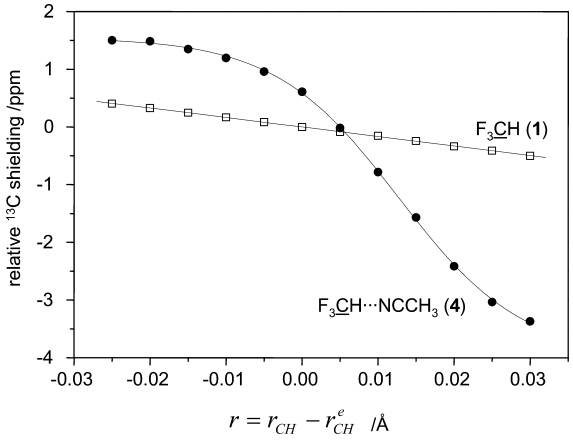

Fig. 6. The calculated (MP2/6–31+G(d, p)) relative shielding constants of ^{13}C nucleus for the free CHF_3 molecule and its complex with acetonitrile as function of the $r = r_{CH} - r_{CH}^{e}$ variable.

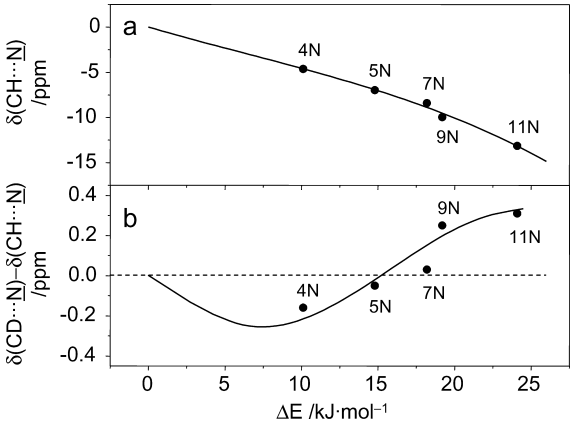

Fig. 7. Experimental values of δ(CH···N) chemical shifts (a) and δ(CD···N) − δ(CH···N) isotope effects (b) plotted versus the calculated interaction energy ΔE, for fluoroform complexes with different bases. Numerical data are taken from Tables 3 and 4.

of perturbation theory implies a decrease of the contribution of the first excited electronic state (which belongs, for these molecules, to the nπ* type) to the ground state, as a result of hydrogen bond formation or even protonation of the nitrogen atom.

The curve, δ(CH···N) = $f(\Delta E)$, displays no peculiarity in the region of the blue-shift/red-shift transformation. A strong NMR criterion, which permits to distinguish between the two cases, was found to be the sign of the H/D isotope effect on the chemical shift of a ^{15}N nucleus of a partner base, transmitted across

a hydrogen bond (see Fig. 7b). Namely, H/D replacement in the neighbouring CHF_3 molecule causes some shielding of the nitrogen nucleus in the case of the blue-shifting H-bonds (e.g., in nitriles **4N** and **5N**) and some nitrogen deshielding for red-shifting H-bonds (in pyridines **9N** and **11N**). A tentative explanation is as follows. The primary effect of H/D replacement is some effective CH bond contraction, due to a decrease of the zero point amplitude of the deuteron vibration in the asymmetric anharmonic potential well. It seems evident that for red-shifting H-bonding this effect must be accompanied by hydrogen bond lengthening (weakening), and for blue-shifting bonding with hydrogen bond shortening (strengthening). In other words, the coupling between the covalent and hydrogen bonds causes opposite effects on the length of a hydrogen bond, depending on its type. As a result, the nitrogen shielding being sensitive mainly to the H···N bond length, decreases or increases upon H/D replacement.

4.3 Estimation of NMR H/D isotope effects

For a semi-quantitative estimation of the measured NMR H/D isotope effects on ^{13}C and ^{15}N chemical shifts, we have used the simplest model, taking the carbon shielding as a function of $r = r_{CH} - r_{CH}^{e}$ and the nitrogen shielding as a function of $R = R_{CN} - R_{CN}^{e}$. Neglecting the population of excited states of the CH stretching vibration we can write [31]:

$$\begin{aligned}
&\delta(\underline{\mathrm{C}}\mathrm{D}\cdots\mathrm{N}) - \delta(\underline{\mathrm{C}}\mathrm{H}\cdots\mathrm{N}) = \\
&\left(\frac{\partial\delta(\underline{\mathrm{C}}\mathrm{H}\cdots\mathrm{N})}{\partial r}\right)_e \Delta_{DH}\langle r\rangle_0 + \frac{1}{2}\left(\frac{\partial^2\delta(\underline{\mathrm{C}}\mathrm{H}\cdots\mathrm{N})}{\partial r^2}\right)_e \Delta_{DH}\langle r^2\rangle_0 + \ldots \\
&\delta(\mathrm{CD}\cdots\underline{\mathrm{N}}) - \delta(\mathrm{CH}\cdots\underline{\mathrm{N}}) = \\
&\left(\frac{\partial\delta(\mathrm{CH}\cdots\underline{\mathrm{N}})}{\partial R}\right)_e \Delta_{DH}\langle R\rangle_0 + \frac{1}{2}\left(\frac{\partial^2\delta(\mathrm{CH}\cdots\underline{\mathrm{N}})}{\partial R^2}\right)_e \Delta_{DH}\langle R^2\rangle_0 + \ldots ,
\end{aligned} \tag{1}$$

where the indices e, 0 refer to the equilibrium and ground states, respectively. The sign Δ_{DH} refers to the H/D isotope effect on the corresponding variable. The ground state expectations $\langle r \rangle_0$, $\langle r^2 \rangle_0$, $\langle R \rangle_0$ and $\langle R^2 \rangle_0$ can be estimated within the framework of a simple linear three-mass model by Sokolov et al. [21] using the following two-dimensional potential function:

$$V = \frac{1}{2}k_{rr}r^2 + \frac{1}{2}k_{RR}R^2 + k_{rR}rR + k_{rrr}r^3 , \tag{2}$$

where k_{rr}, k_{rR} and k_{RR} are the harmonic force constants, and k_{rrr} is the cubic force constant of the CH bond. The solution of the harmonic vibrational problem with this potential (without the last term) gives the exact values of the harmonic frequencies for the stretching CH (ν_1) and CN (ν_σ) vibrations:

$$\begin{aligned}
\nu_1 &= \frac{1}{2\pi c}\sqrt{\frac{k_{rr}}{\mu_1}}\left(1 + \frac{\mu_1}{\mu_\sigma}\frac{k_{rR}}{k_{rr}}\right) \\
\nu_\sigma &= \frac{1}{2\pi c}\sqrt{\frac{k_{RR}}{\mu_\sigma}}\left(1 - \frac{k_{rR}^2}{2k_{rr}k_{RR}}\right),
\end{aligned} \tag{3}$$

where μ_1 and μ_σ are the reduced masses of the two vibrations. For the mean values of the squares of the r and R variables (or square quantum-mechanical amplitudes in the ground vibrational state), the following equations apply (the anharmonic corrections for these values can be neglected) [22]:

$$\begin{aligned} \left\langle r^2 \right\rangle_0 &= \frac{1}{2} hc\nu_1 k_{rr}^{-1} \\ \left\langle R^2 \right\rangle_0 &= \frac{1}{2} hc\nu_\sigma k_{RR}^{-1} . \end{aligned} \tag{4}$$

The account of the cubic term using perturbation theory gives (in second order) negative additions to the harmonic frequencies and (in first order) the following equations for the expectations of r and R in the ground vibrational state:

$$\begin{aligned} \langle r \rangle_0 &= -\frac{3}{2} hc\nu_1 \frac{k_{rrr}}{k_{rr}^2} \\ \langle R \rangle_0 &= \frac{3}{2} hc\nu_1 \frac{k_{rrr}}{k_{rr}^2} \frac{k_{rR}}{k_{RR}} . \end{aligned} \tag{5}$$

Here the diagonal force constants k_{rr} and k_{RR} are always positive, the cubic constant k_{rrr} is negative, and the off-diagonal constant, k_{rR}, describing the dynamic coupling of two bonds, can be either positive or negative, depending on the type of a given hydrogen bond. The only parameter in Eq. (5) depending on reduced mass is the harmonic frequency, ν_1, which decreases on H/D replacement approximately by the factor $\sqrt{2}$.

Combining Eqs. (1), (4), (5), the following equations for the H/D NMR isotope effects can be derived:

$$\begin{aligned} &\delta\left(\underline{\mathrm{C}}\mathrm{D}\cdots\mathrm{N}\right) - \delta\left(\underline{\mathrm{C}}\mathrm{H}\cdots\mathrm{N}\right) = \\ &hc\Delta_{DH}\nu_1 \left[\frac{1}{4} \left(\frac{\partial^2 \delta\left(\underline{\mathrm{C}}\mathrm{H}\cdots\mathrm{N}\right)}{\partial r^2} \right)_e k_{rr}^{-1} - \frac{3}{2} \left(\frac{\partial \delta\left(\underline{\mathrm{C}}\mathrm{H}\cdots\mathrm{N}\right)}{\partial r} \right)_e \frac{k_{rrr}}{k_{rr}^2} \right], \end{aligned} \tag{6}$$

$$\begin{aligned} &\delta\left(\mathrm{CD}\cdots\underline{\mathrm{N}}\right) - \delta\left(\mathrm{CH}\cdots\underline{\mathrm{N}}\right) = \\ &\left(\frac{\partial \delta\left(\mathrm{CH}\cdots\underline{\mathrm{N}}\right)}{\partial R} \right)_e \Delta_{DH} \langle R \rangle_0 = \frac{3}{2} hc\Delta_{DH}\nu_1 \left(\frac{\partial \delta\left(\mathrm{CH}\cdots\underline{\mathrm{N}}\right)}{\partial R} \right)_e \frac{k_{rrr} k_{rR}}{k_{rr}^2 k_{RR}} . \end{aligned} \tag{7}$$

(In Eq. (7), the term containing the second derivative, $\left(\frac{\partial^2 \delta(\mathrm{CH}\cdots\underline{\mathrm{N}})}{\partial R^2} \right)_e$, was omitted, because the harmonic frequency ν_σ and amplitude $\langle R^2 \rangle_0$ for the hydrogen bond vibration are practically insensitive to H/D substitution.)

All the needed constants in Eqs. (6) and (7) can, in principle, be calculated *ab initio*. However, in practical computations we faced the following problem. The procedure of normal mode analysis, included in the program package, Gaus-

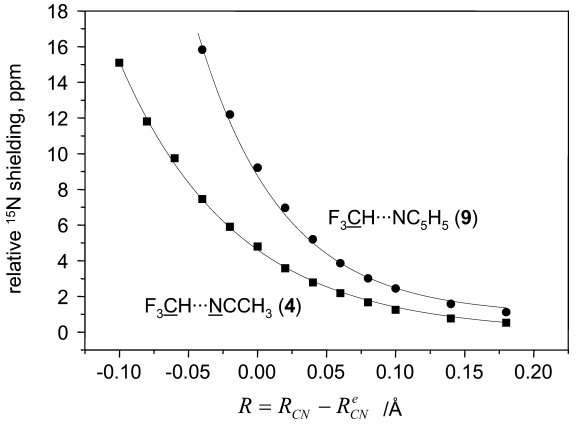

Fig. 8. The calculated (MP2/6–31+G(d, p)) dependencies of the relative ^{15}N shielding constant on an internal variable, describing the stretching hydrogen bond vibration, $R = R_{CH} - R_{CH}^e$, for complexes of fluoroform with acetonitrile (**4**) and pyridine (**9**).

sian 98, reproduces very poorly the values of three lowest (intermolecular) frequencies of weakly hydrogen bonded complexes. The result depends strongly on the level of electron correlation account and the used basis set. Thus, the *ab initio* estimation of the values k_{rR} and k_{RR} cannot be reliable. At the same time, the shapes of the computed curves $R = f(r)$ depend weakly on the basis set. That is why for evaluating the H/D isotope effect on the ^{15}N chemical shift, we have used only the indirect form of Eq. (1), involving the mutual dependence of two vibrational variables, r and R [28]:

$$\delta\left(\mathrm{CD}\cdots\underline{\mathrm{N}}\right)-\delta\left(\mathrm{CH}\cdots\underline{\mathrm{N}}\right)=\left(\frac{\partial\delta\left(\mathrm{CH}\cdots\underline{\mathrm{N}}\right)}{\partial R}\right)_e\Delta_{DH}\left\langle R\right\rangle_0=$$
$$\left(\frac{\partial\delta\left(\mathrm{CH}\cdots\underline{\mathrm{N}}\right)}{\partial R}\right)_e\left[\left(\frac{\partial R}{\partial r}\right)_e\Delta_{DH}\left\langle r\right\rangle_0+\frac{1}{2}\left(\frac{\partial^2 R}{\partial r^2}\right)_e\Delta_{DH}\left\langle r^2\right\rangle_0\right]. \quad (8)$$

This leads to the final expression:

$$\delta\left(\mathrm{CD}\cdots\underline{\mathrm{N}}\right)-\delta\left(\mathrm{CH}\cdots\underline{\mathrm{N}}\right)=$$
$$hc\Delta_{DH}\nu_1\left(\frac{\partial\delta\left(\mathrm{CH}\cdots\underline{\mathrm{N}}\right)}{\partial R}\right)_e\left[\frac{1}{2}\left(\frac{\partial^2 R}{\partial r^2}\right)_e k_{rr}^{-1}-\frac{3}{2}\left(\frac{\partial R}{\partial r}\right)_e\frac{k_{rrr}}{k_{rr}^2}\right]. \quad (9)$$

The calculated shielding function $\delta(\underline{\mathrm{C}}\mathrm{H}\cdots\mathrm{N}) = f(r)$ for complex **4** is shown in Fig. 6. In Fig. 8 the calculated shielding functions $\delta(\mathrm{CH}\cdots\underline{\mathrm{N}}) = f(R)$ for complexes **4** and **9** are depicted. In Fig. 9 the graph for $R = f(r)$ is plotted, calculated as described in [28]. The derivatives in Eqs. (6), (9) at zero points, obtained from the Figs. 6, 8, and 9, as well as the constants, k_{rrr} and k_{rr}, calculated as described in Experimental section, are listed in Table 7.

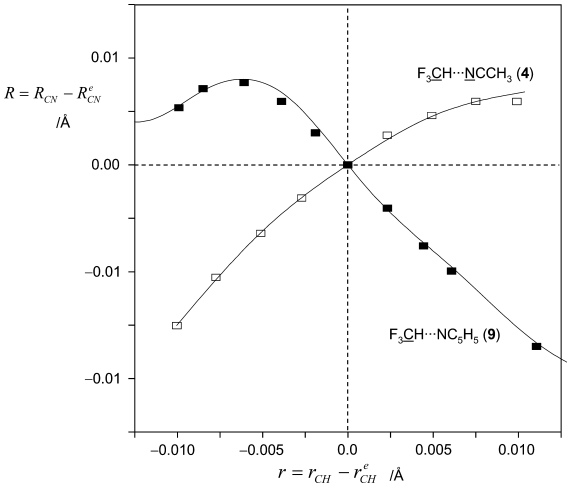

Fig. 9. The calculated mutual dependencies of internal variables $r = r_{CH} - r_{CH}^e$ and $R = R_{CN} - R_{CN}^e$ for complexes of fluoroform with acetonitrile (**4**) and pyridine (**9**).

It can be seen from Fig. 5d that hydrogen substitution by a heavier isotope is accompanied by a carbon shielding, whereas the sign of the isotope effect on the ^{15}N chemical shift is ambiguous and determined by the sign of the dynamic coupling between the covalent and hydrogen bond vibrations (see Fig. 7). This coupling is positive ($k_{rR} > 0$) in the red-shifting case (complex **9**) and is negative ($k_{rR} < 0$) in the blue-shifting case (complex **4**).

The data in Table 7 show that the evaluation of the NMR isotope effects within the simplest one-dimensional model is in surprisingly good accordance with experiment. Taking into account the usual high sensitivity of paramagnetic deshielding of heavy nuclei to angle variables, we cannot exclude, that the involvement of the bending vibration (ν_4 for fluoroform) may destroy the coincidence. The result of a three-dimensional calculation of the NMR isotope effects for two particular complexes, fluoroform-acetonitrile (**4**) and fluoroform-pyridine (**9**), will be published elsewhere. We believe, however, that the above model describes correctly the physical essence of the found inversion of the NMR isotope effect across a hydrogen bond when going from the blue-shifting to red-shifting case. We believe that the origin lies in the inversion of the dynamic coupling of covalent and hydrogen bond vibrations. The main parameter of this coupling, namely, the ratio, k_{rR}/k_{RR}, evaluated from the experimentally derived ^{15}N secondary H/D isotope effect, is given in the last row of Table 7.

It is interesting that the cubic force constant for the CH bond of fluoroform, k_{rrr}, and the H/D isotope effect on the C···H distance are practically insensitive to hydrogen bond formation. At the same time, the value of the secondary NMR isotope effect on the ^{13}C chemical shift increases approximately by a factor of

Table 7. Calculated (MP2/6–31(d, p)) constants required for the model estimation of H/D isotope effects on NMR chemical shifts of complexes of fluoroform with acetonitrile (**4**) and pyridine (**9**).

	F_3CH, **1**	$F_3CH\cdots NCCH_3$, **4**	$F_3CH\cdots NC_5H_5$, **9**
ν_1 /cm^{-1}	3118 (2282)[a]	3122 (2285)[a]	3112 (2278)[a]
k_{rr} /mDyn · Å^{-1}	5.69	5.71	5.66
k_{rrr} /mDyn · Å^{-2}	−4.62	−4.76	−4.84
$\Delta_{DH}\langle r\rangle_0$ /Å	−0.00355	−0.00364	−0.00375
$\Delta_{DH}\langle r^2\rangle_0$ /Å^2	−0.0015	−0.0015	−0.0015
$\left(\frac{\partial\delta(\underline{C}H\cdots N)}{\partial r}\right)_e$ /ppm · Å^{-1}	19.0	53.3	83.3
$\left(\frac{\partial^2\delta(\underline{C}H\cdots N)}{\partial r^2}\right)_e$ /ppm · Å^{-2}	57	64	72
$\left(\frac{\partial\delta(CH\cdots\underline{N})}{\partial R}\right)_e$ /ppm · Å^{-1}		61.2	108.9
$\left(\frac{\partial R}{\partial r}\right)_e$		+1.2	−1.4
$\left(\frac{\partial^2 R}{\partial r^2}\right)_e$ /Å^{-1}		−1.6	+1.2
$\delta(\underline{C}D\cdots N) - \delta(\underline{C}H\cdots N)$ /ppm	−0.11 (−0.22)[b]	−0.24 (−0.28)[b]	−0.37 (−0.36)[b]
$\delta(CD\cdots\underline{N}) - \delta(CH\cdots\underline{N})$ /ppm		−0.12 (−0.16)[b]	+0.36 (+0.25)[b]
$\frac{k_{rR}}{k_{RR}}$		−0.71	+1.0

a - in brackets calculated harmonic frequencies for the isotopic form $F_3{}^{13}C^2H$.
b - in brackets experimental values.

two when going from the free CHF_3 molecule to its complex with 2, 4, 6-Me_3-C_5H_2N (**11**) (Table 2). In the present treatment, this increase originates from the rise of shielding sensitivity to the C···H distance with hydrogen bond strength. The physical reason of this effect is so far unclear.

5 Conclusions

We have studied hydrogen bonded complexes formed by CHF_3 with various proton acceptors in solution. According to the literature, in this series the increase of the proton accepting ability of the partner molecule leads to the transition from the blue- to red-shifting hydrogen bond. As a measure of proton accepting ability we have chosen the *ab initio* calculated H-bond interaction energy ΔE. We have demonstrated that most of the experimental NMR parameters do not show any qualitative changes upon transition from blue- to red-shifting hydrogen

bond. The exception is the H/D isotope effect on ^{15}N shielding of the partner molecule, which changes its sign. We have rationalized this finding by performing *ab initio* calculations of the C···N = *f*(C···H) dependence. It appears that the unusual sign of the H/D isotope effect on ^{15}N chemical shift across a blue-shifting H-bond can be explained as a result of the inversion of the dynamic coupling of the covalent and hydrogen bond vibrations.

Acknowledgement

This work is supported by Russian Foundation for Basic Research (grant No. 08–03-00615). S.M. thanks the DAAD for a postdoctoral grant, D/03/18809.

References

1. B. J. van der Veken, W. A. Herrebout, R. Szostak, D. N. Shchepkin, Z. Havlas, P. Hobza, J. Am. Chem. Soc. **123** (2001) 12290.
2. I. E. Boldeskul, I. F. Tsymbal, E. V. Ryltsev, Z. Latajka, A. J. Barnes, J. Mol. Struct. **436** (1997) 167.
3. S. N. Delanoye, W. A. Herrebout, B. J. van der Veken, J. Am. Chem. Soc. **124** (2002) 11854.
4. S. M. Melikova, K. S. Rutkowski, P. Rodziewicz, A. Koll, Chem. Phys. Lett. **352** (2002) 301.
5. P. Hobza, V. Spirko, Z. Havlas, K. Buchhold, B. Reinmann, H. D. Barth, B. Brutschy, Chem. Phys. Lett. **299** (1999) 180.
6. K. S. Rutkowski, W. A. Herrebout, S. M. Melikova, P. Rodziewicz, B. J. van der Veken, A. Koll, Spectr. Acta **A61** (2005) 1595.
7. A. J. Barnes, J. Mol. Struct. **704** (2004) 3.
8. K. S. Rutkowski, P. Rodziewicz, S. M. Melikova, W. A. Herrebout, B. J. van der Veken, A. Koll, Chem. Phys. **313** (2005) 225.
9. W. A. Herrebout, S. M. Melikova, S. N. Delanoye, K. S. Rutkowski, D. N. Shchepkin, B. J. van der Veken, J. Phys. Chem. A **109** (2005) 3038.
10. W. Zierkiewicz, D. Michalska, Z. Havlas, P. Hobza, ChemPhysChem **3** (2002) 511.
11. J. M. Fan, L. Liu, Q. X. Guo, Chem. Phys. Lett. **365** (2002) 464.
12. V. V. Bertsev, N. S. Golubev, D. N. Shchepkin, Opt. Spectrosc. **68** (1977) 951 (Russian).
13. P. Hobza, Z. Havlas, Chem. Phys. Lett. **303** (1999) 447.
14. P. Hobza, Z. Havlas, Chem. Rev. **100** (2000) 4253.
15. Y. Gu, T. Kar, S. Scheiner, J. Am. Chem. Soc. **121** (1999) 9411.
16. K. Hermansson, J. Phys. Chem. A **106** (2002) 4695.
17. L. Pejov, K. Hermansson, J. Chem. Phys. **119** (2003) 313.
18. G. A. Jeffrey, J. Mol. Struct. **485** (1999) 293.
19. E. Cubero, M. Orozco, P. Hobza, F. J. Luque, J. Phys. Chem. A **103** (1999) 6394.
20. S. M. Melikova, K. S. Rutkowski, P. Rodziewicz, A. Koll, J. Mol. Struct. **705** (2004) 49.
21. N. D. Sokolov, V. A. Savel'ev, Chem. Phys. **22** (1977) 383.
22. D. N. Shchepkin, *Anharmonicity Effects in the Spectra of Hydrogen-Bonded Complexes.* Dep. VINITI N 7511-B87, Russian (1987).
23. a) J. D. LaZerte, L. J. Hals, T. S. Reid, G. H. Smith, J. Am. Chem. Soc. **75** (1953) 4525. b) M. Hudlicky, *Chemistry of Organic Fluorine Compounds*. 2nd (revised) edition, Halsted Press (1976) p. 499.

24. a) T. W. Whaley, D. G. Ott, J. Labelled Compd. Rad. **10** (1974) 283. b) A. T. Balaban, A. J. Boulton, D. G. McMahan, G. H. E. Baumgarten, Org. Synth. Coll. **5** (1973) 1112. c) N. S. Golubev, S. N. Smirnov, P. Schah-Mohammedi, I. G. Shenderovich, G. S. Denisov, V. A. Gindin, H. H. Limbach, Russ. J. Gen. Chem. **67** (1997) 1082. d) V. N. Bocharov, S. F. Bureiko, N. S. Golubev, Sh. S. Shajakhmedov, J. Mol. Struct. **444** (1998) 57.
25. C. Weygand, G. Hilgetag, *Organisch-Chemische Experimentier Kunst*. 4th edition, Johann Ambrosius Barth (1970) p.533.
26. S. N. Smirnov, N. S. Golubev, G. S. Denisov, H. Benedict, P. Schah-Mohammedi, H.-H. Limbach, J. Am. Chem. Soc. **118** (1996) 4094.
27. M. J. Frisch, G. W. Trucks, H. B. Schlegel, G. E. Scuseria, M. A. Robb, J. R. Cheeseman, V. G. Zakrzewski, J. A. Montgomery, R. E. Stratmann, J. C. Burant, S. Dapprich, J. M. Millam, A. D. Daniels, K. N. Kudin, M. C. Strain, O. Farkas, J. Tomasi, J. V. Barone, M. Cossi, R. Cammi, B. Mennucci, C. Pomelli, C. Adamo, S. Clifford, J. G. Ochterski, G. A. Petersson, P. Y. Ayala, G. Cui, K. Morokuma, D. K. Malick, A. D. Rabuck, K. Raghavachari, J. B. Foresman, J. Cioslowski, J. V. Ortiz, B. B. Stefanov, G. Liu, A. Liashenko, P. Piskorz, L. Komaromi, R. Gomperts, R. L. Martin, D. J. Fox, T. Keith, M. A. Al-Laham, C. Y. Peng, A. Nanayakkara, C. Gonzalez, M. Challacombe, P. M. W. Gill, B. G. Johnson, W. Chen, M. W. Wong, J. L. Andres, M. Head-Gordon, E. S. Replogle, J. A. Pople, Gaussian 98 (Revision A.7), Gaussian, Inc., Pittsburgh, PA (1988).
28. N. S. Golubev, S. M. Melikova, D. N. Shchepkin, I. G. Shenderovich, P. M. Tolstoy, G. S. Denisov, Z. Phys. Chem. **217** (2003) 1549.
29. P. Rodziewicz, K. S. Rutkowski, S. M. Melikova, A. Koll, ChemPhysChem. **6** (2005) 1282.
30. G. Martin, M. L. Martin, J. P. Gouesnard, *^{15}N NMR Spectroscopy. In: NMR Basic Principles and Progress*. Heidelberg: Springer (1989) V.18. 322 pp.
31. R. D. Wigglesworth, W. T. Raynes, S. Kirpekar, J. Oddershede, S. P. A. Sauer, J. Chem. Phys. **112** (2000) 736.